

Rotary motion of a micro-solid particle under a stationary difference of electric potential

Tomo Kurimura,¹ Seori Mori,² Masako Miki,² and Kenichi Yoshikawa^{2,a)}

¹Department of Physics, Kyoto University, Kyoto 606-8502, Japan

²Faculty of Life and Medical Sciences, Doshisha University, Kyotanabe, Kyoto 610-0394, Japan

(Received 29 February 2016; accepted 27 June 2016; published online 18 July 2016)

The periodic rotary motion of spherical sub-millimeter-sized plastic objects is generated under a direct-current electric field in an oil phase containing a small amount of anionic or cationic surfactant. Twin-rotary motion is observed between a pair of counter-electrodes; i.e., two vortices are generated simultaneously, where the line between the centers of rotation lies perpendicular to the line between the tips of the electrodes. Interestingly, this twin rotational motion switches to the reverse direction when an anionic surfactant is replaced by a cationic surfactant. We discuss the mechanism of this self-rotary motion in terms of convective motion in the oil phase where nanometer-sized inverted micelles exist. The reversal of the direction of rotation between anionic and cationic surfactants is attributable to the difference in the charge sign of inverted micelles with surfactants. We show that the essential features in the experimental trends can be reproduced through a simple theoretical model, which supports the validity of the above mechanism. © 2016 Author(s). All article content, except where otherwise noted, is licensed under a Creative Commons Attribution (CC BY) license (<http://creativecommons.org/licenses/by/4.0/>). [<http://dx.doi.org/10.1063/1.4958657>]

I. INTRODUCTION

Living organisms convert electrical potential, or membrane potential, to kinetic energy.¹ They exhibit the features of a molecular engine by dissipating the chemical potential or through an electrochemical gradient across the membrane, such as in the movement of bacterial flagella and the rotation of ATPase. Thus, biological molecular motors with a characteristic size on the order of nanometers operate under a stationary direct current (DC) voltage.² Despite these examples in Nature, it is still difficult to fabricate electrical motors on a sub-millimeter scale.

Recently, it was found that a microscopic water droplet undergoes oscillatory motion between sharp-point electrodes under stationary DC voltage.³ Numerous studies^{3–13} have reported various modes of droplet motion between electrodes using both experimental and numerical methods. A droplet behaves as an electrical charge-carrier between a pair of electrodes in an oil medium as an insulator. When a droplet is on or near one of the electrodes, it gains a charge and is then pulled toward the opposite electrode. As the droplet reaches the opposite electrode, its charge is reversed, and the droplet moves back. Such back-and-forth motion of the droplet repeats periodically under a stationary DC voltage. The oscillatory properties of this motion, such as its periodicity and trajectory, are critically dependent on the physicochemical conditions. For example, the chemical nature of the liquid inside the droplet,^{9,10} the geometry of the electrodes,¹¹ and the presence of surfactants¹² all influence the mode of dynamic motion of the droplet.

In the present article, we report our new findings on the generation of regular motion of a solid sub-millimeter-sized plastic object under a stationary DC electrical field. Interestingly, a twin-whirl rotary motion is observed for the solid object, in contrast to the back-and-forth oscillatory motion for a water droplet, between facing sharp-point electrodes situated along a line. The mechanism of the generation of such interesting regular motion will be discussed along with the effect of a coexisting surfactant in the oil phase. We propose a scenario in which stable rotary advection of the fluidic solution emerges under a DC field and this causes orbital motion of the solid object. We also report the results of a numerical simulation with a simple fluid equation, which reproduces the essential features of the experimental trend.

II. MATERIALS AND METHODS

A schematic illustration of the experimental setup is shown in Fig. 1. Polyethylene particles (Sumitomo Seika Chemicals Co., Japan) were suspended in silicone oil (KF-56, Shin-Etsu Chemical Co., Japan) containing 0.5 M or 0.65 M surfactant; an anionic surfactant, di-(2-ethylhexyl)phosphoric acid (237825, Sigma-Aldrich Co., USA) or a cationic surfactant, di-(2-ethylhexyl)amine (351-00202, Wako Pure Chemical Industries, Ltd., Japan). We obtained a homogeneous oil phase through mechanical agitation with a vortex mixer for 1 min. A droplet of this silicone oil containing particles was placed on a glass slide, and constant voltage was applied to the droplet using cone-shaped tungsten electrodes. The motion of plastic particles within the droplet was observed by using an optical microscope (IX71, Olympus Co., Japan).

^{a)}Electronic mail: keyoshik@mail.doshisha.ac.jp



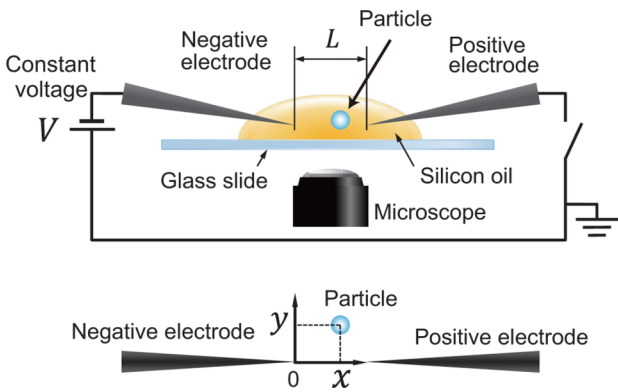


FIG. 1. Schematic representation of the experimental setup. Stationary DC voltage was applied between a pair of tapered tungsten electrodes inserted into silicone oil containing polyethylene micro-particles.

III. RESULTS

Figure 2 shows examples of the rotary motion of numerous plastic particles. Twin whirls are generated on both sides of the line between the pair of tapered electrodes, and the rotations are in opposite directions with respect to each other. The existence of a pair of whirls suggests that the rotary motions of particles are driven under the cyclic flow

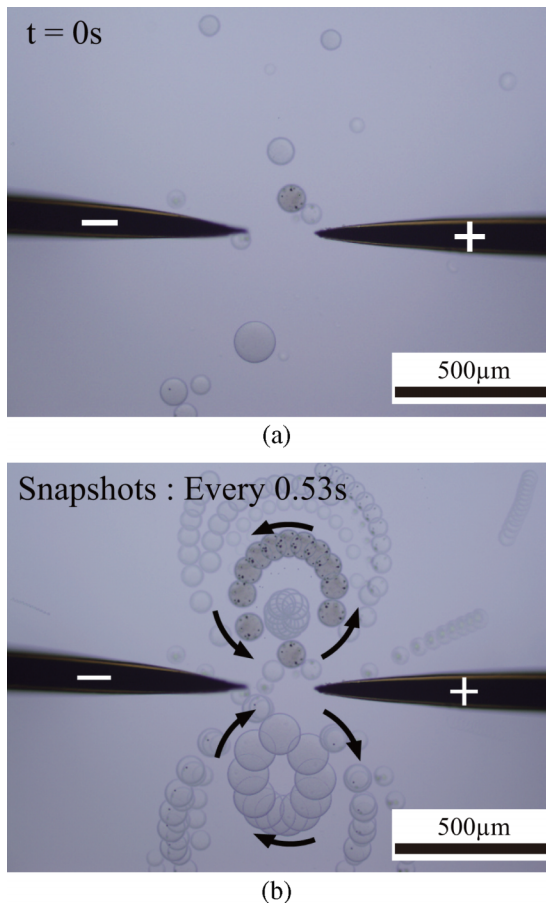


FIG. 2. Self-revolution of plastic particles. (a) Initial condition at $t = 0$ s from when DC voltage was applied. (b) Overlap of snapshots every 0.53 s. Multiple polyethylene particles with radii of $r = 50\text{--}175\ \mu\text{m}$ rotate in the oil phase with an anionic surfactant at $V = 170$ V.

of the bulk oil phase. A pair of rotary motions of this type has not been observed for the motion of water droplets under constant DC voltage, although both single cyclic motion and back-and-forth motion have been reported. We also performed the experiments with the different concentration of the anionic surfactant; 0 M and 0.1 M. We confirmed that, under these experimental conditions, rotary motion of this type is not generated (See the supplementary material¹⁴). These results suggest that the rotational motion of plastic particles is caused by the flow in the oil phase containing charged reverse micelles.

Figure 3(a-2) shows the angular velocity of the particle vs. the position angle during one period of revolution. We defined the position angle as follows (this is also shown in Fig. 3(a-1)). When the particle is closest to and farthest from the positive electrode, the position angle θ is π and 0, respectively. The particle has a maximum angular velocity when it moves from the negative electrode to the positive electrode.

We show the experimental results with an anionic surfactant. Figure 3(b) shows the rotary motion of the particle when we used a cationic surfactant instead of the anionic surfactant. In this case, the direction of the revolving motion is opposite that with the anionic surfactant. We confirmed that rotary motion of this type is never generated in the absence of a cationic/anionic surfactant.

In the above experiments on rotary motion, we used anionic and cationic surfactants with a rather bulky hydrophobic group. It has been well established in colloid

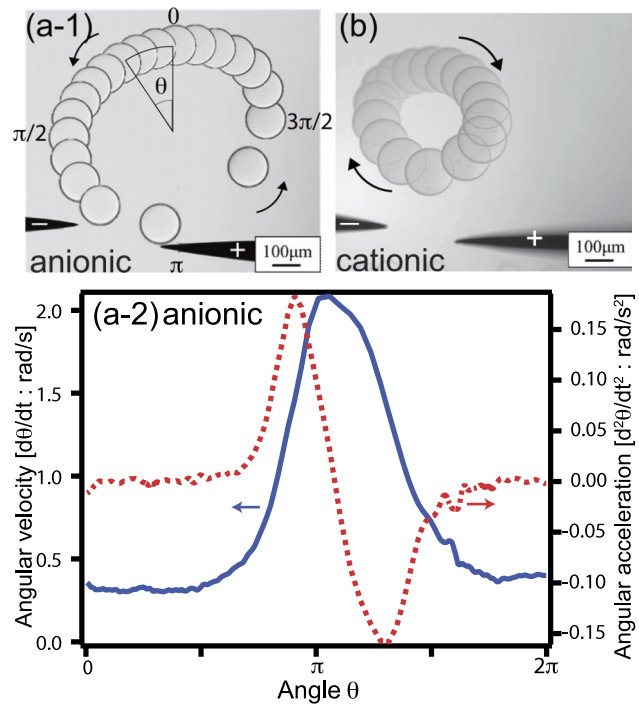


FIG. 3. ((a-1) and (b)): Angular velocity and angular acceleration depending on the angular position of the particle in the presence of an anionic surfactant (a-1), or a cationic surfactant (b). (a-2): The blue solid line is the velocity and the red dotted line is the acceleration. Videos of these experiments are shown in the supplementary material.¹⁴ The radius of rotation in both the anionic and cationic surfactants depends on the initial position of a particle. Particle size: $d = 175\ \mu\text{m}$. Applied voltage: $V = 170$ V and 180 V for (a) and (b), respectively.

chemistry that a surfactant with a bulky group forms inverted micelles in an oil phase, where the characteristic size, on the order of 10-100 nm, is much smaller than the optical wavelength. Thus, inverted micelles of such small sizes are usually transparent to optical light.

The switching of the direction of rotation between anionic and cationic surfactants is attributable to the inversion of the electrical charge of the inverted micelles together with the sign inversion of the charge of the counter-ions. Due to symmetry breaking between relatively large inverted micelles with multiple electrical charges and multiple small counter-ions, we can expect the generation of a net electrical current between the pair of electrodes under stationary DC voltage. For example, in the experiment with anionic surfactant, negatively charged inverted micelles are formed in the solution. These negatively charged inverted micelles are thought to act as a charge carrier, i.e., negative charge is transferred from the negative electrode to the positive electrode. The reverse situation occurs for inverted micelles with a cationic surfactant. Recall that rotary motion of this type was not generated in the absence of a cationic/anionic surfactant.

Based on repeated measurements, we found that the primary factor that determines the radius of rotation is the initial position of the particle when we begin to apply the DC voltage. This suggests that the scroll flow of the bulk solution containing cationic/anionic surfactant plays an essential role.

IV. NUMERICAL MODELING

To extract the essence of the underlying mechanism, we assume that the homogeneous bulk phase contains invisible inverted micelles that act as electrical charge carriers; i.e., inverted micelles exhibit a relatively large electrical charge accompanied by counter-ions with the opposite sign. The marked asymmetry in geometrical size and charge number between the inverted micelle and counter-ions would result in the generation of a net electrical current under DC voltage. Thus, we assume that the medium containing inverted micelles can carry electrical charge between the electrodes under stationary voltage. Here, we adapt the Stokes equation by including a continuous condition of charge density

$$\frac{\partial \mathbf{u}}{\partial t} + (\mathbf{u} \cdot \nabla) \mathbf{u} = -\nabla p + \frac{1}{Re} \nabla^2 \mathbf{u} + \mathbf{E} \rho_e, \quad (1)$$

where \mathbf{u} is the velocity of the fluid and p is the pressure. \mathbf{E} is the electrical field. ρ_e is the effective charge density, which reflects the large difference in mobility between the inverted micelle and surrounding counter-ions with the opposite electrical charge.

Since the Reynolds number (Re) in our experiment is around 10^{-8} , we can neglect the inertia term from Eq. (1) and obtain

$$\frac{\partial \mathbf{u}}{\partial t} = -\nabla p + \frac{1}{Re} \nabla^2 \mathbf{u} + \mathbf{E} \rho_e. \quad (2)$$

With regard to the time-dependent change in the charge density, we adopt the following equation, where ρ_e is the charge density for a unit volume. The time-development of

the charge density can be written as

$$\frac{\partial \rho_e}{\partial t} + \nabla \cdot (\rho_e \mathbf{u}) = (\sigma + \rho_e \mu) \Delta \phi, \quad (3)$$

where σ is the conductivity, μ is the permittivity of the fluid. ϕ is the electric potential, where $\mathbf{E} = -\nabla \phi$.

With the electrode configuration in the present study, near each electrode, nm-sized inverted micelles tend to be charged with an electrical potential that is the same sign as that of the electrode. We assume that the medium proximal to the electrode then accepts the charge from the contacting electrode.

To obtain a spatial profile of the electrical field under DC potential, we solve the Poisson equation under the following conditions. The area for the calculation is 50×50 . The electrodes are located at $(x, y) = (0-20, 24-26)$, and $(30-50, 24-26)$. The positions and shapes are shown in Fig. 4(a). The negative electrode is on the left and the positive electrode is on the right. When we calculate the Poisson equation, the potential difference is fixed at unity. We deduce an electrical field through the procedure with a scaled electric field. We run the Stokes equation by using the scaled electric field and then show the result after rescaling to the actual electric field.

In the simulation, the distance between grid points corresponds to ca. $100 \mu\text{m}$ which is comparable to that in the actual experimental system in Fig. 1, whereas the time step corresponds to 0.005 s. As for the effect of the electrical sign of the head group of the surfactant, we consider the

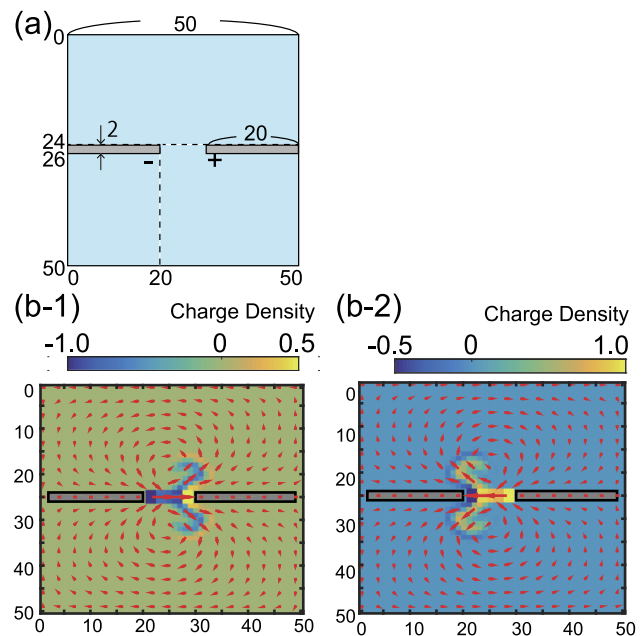


FIG. 4. (a) Geometry adopted for the numerical simulation with a pair of electrodes (gray rectangles) and a fluidic region (blue). The numbers correspond to pixel numbers. The boundary condition is taken as no-flux for simplicity. ((b-1) and (b-2)) Numerical results for the flow profile after the application of DC voltage ($t = 1.5$ s). The colors reflect the charge density in the solution as indicated by the color bar at the top, except for the metal electrode. The red arrows indicate the velocity of the liquid. (b-1) Model of the experiment with an anionic surfactant. (b-2) Model of the experiment with a cationic surfactant.

difference in electrical charge, or the change in ρ_e around the electrodes.

Next, we calculated the Stokes equation. The periphery is considered to be a wall that is far enough away that it does not affect the flow around the electrodes. The border of the electrode is also considered a non-slip wall. Thus, as a boundary condition at the border of the electrode, we set the pressure gradient to zero to realize a non-flux condition. The parameters were set to $Re = 0.05$, $\sigma = 1.0e^{-8}$, and $\mu = 1.0e^{-7}$. In our preliminary simulation so as to reduce the computational time, we have adopted a relatively large Re , in comparison with that in our actual experimental system, to check for the presence of each of the two vortices. The charge density at the positive electrode is fixed at 1.0, and that at the negative electrode is fixed at -0.5 in Fig. 4(b-1). In the case of Fig. 4(b-2), that at the positive electrode is fixed at 0.5, and that at the negative electrode is fixed at -1.0 . At the beginning of the calculation, the liquid near the electrodes is charged. Thereafter, the charged liquid is driven by the electrical field between the electrodes, and rotary motion of the liquid is generated. We consider that the amount of negative charge is greater than the amount of positive charge when an anionic surfactant is added to the oil, and this relationship is reversed when a cationic surfactant is added. This difference explains the reverse direction of rotation. These consequences are shown in Figs. 4(b-1) and 4(b-2). In the present simulation, we have not adopted a strict conservation of the integrated charge density. We confirmed that this non-conservative condition has only a minimal effect on the numerical simulation for the period of time given in Figs. 4(b-1) and 4(b-2). The results of this numerical study suggest that charging of the bulk oil phase plays an essential role in the twin vortices of solid particles observed in the experiments (Figs. 2 and 3). Under the numerical conditions in the present study, we found that twin vortices appear as a metastable state. Further detailed numerical studies will be needed to reproduce the flow profiles in a more precise manner.

V. DISCUSSION

In our experiment, we observed twin vortices in the rotary motion of plastic particles under stationary DC voltage. In past studies on the motion of a water droplet, such twin rotary motion has never been observed. Plastic particles are dielectric, and their dielectric constant is smaller than that of water. When we put a dielectric material under an electric field, its inductive dipole moment is in the direction of the electric field. When there are many plastic particles, the particles gather and link together because of their dipole interaction.¹⁵ Under a uniform electric field, they stop once their dipole moment is in the direction of the field. If they are under a non-uniform field, they are driven by the dielectrophoretic force along the gradient of the electric field. Without a charge, the particle stops at the electrode. For this reason, we consider that charging of the oil phase containing a cationic/anionic surfactant plays an essential role in the generation of the twin vortices of solid particles. Rotary motion is evidently the result of convective rolling under a DC electric field, suggesting that the mechanism is somewhat similar to that in the so-called EHD flow.^{16,17} There have been some reports that

a dielectric liquid containing various additives flows under an electrical field.^{18,19} In the present article, we have shown that, under a stationary DC field, not only convective directional flow but also regular rotary motion is generated. It may be possible to move a micrometer-sized object driven by the generated fluidic flow. Especially, it is tempting to extend the observation of spherical solid particles to objects of various geometries. It should be possible to generate microscopic spinning together with orbital motion for a solid particle with suitable symmetry breaking of the spherical geometry, for example, by introducing a propeller-shaped object. It would also be interesting to apply this EHD as a new type of electronic pump. By changing the spatial symmetry around the pair of electrodes, we may change the system to cause single-vortex flow. For example, by introducing a solid wall on either side of the pair of electrodes, it may become possible to induce a single rolling fluidic current.

ACKNOWLEDGMENTS

This work was partly supported by KAKENHI, Grants-in-Aid for Scientific Research, Grant Nos. 15H02121, 16K13655 and 25103012. This work was also supported by a JSPS Grant-in-Aid for JSPS Fellows, Grant No. 15J02049. We would like to thank Professor A. Shioi and Dr. D. Yamamoto at Doshisha University, Dr. M. Takinoue at Tokyo Technology, and Dr. M. Ichikawa at Kyoto University for their fruitful discussions.

- ¹R. M. Berry and J. P. Armitage, *Adv. Microb. Physiol.* **41**, 291-337 (1999); G. Lowe, M. Meister, and H. C. Berg, *Nature* **325**, 637-640 (1987); Y. Magariyama, S. Sugiyama, K. Muramoto, Y. Maekawa, I. Kawagishi, Y. Imae, and S. Kudo, *ibid.* **371**, 752 (1994); M. Silverman and M. Simon, *ibid.* **249**, 7374 (1974); R. Yasuda, H. Noji, K. Kinoshita, Jr., and M. Yoshida, *Cell* **93**, 1117-1124 (1998); P. D. Boyer, *Annu. Rev. Biochem.* **66**, 717749 (1997).
- ²O. E. Perelstein, V. A. Ivanov, Y. S. Velichko, P. G. Khalatur, A. R. Khokhlov, and I. I. Potemkin, *Macromol. Rapid Commun.* **28**, 977980 (2007).
- ³M. Hase, S. N. Watanabe, and K. Yoshikawa, *Phys. Rev. E* **74**, 046301 (2006).
- ⁴P. Beranek, R. Flittner, V. Hrobar, P. Ethgen, and M. Pribyl, *AIP Adv.* **4**, 067103 (2014).
- ⁵D. J. Im, B. S. Yoo, M. M. Ahn, D. Moon, and I. S. Kang, *Anal. Chem.* **85**, 4038-4044 (2013).
- ⁶D. W. Lee, D. J. Im, and I. S. Kang, *Appl. Phys. Lett.* **100**, 221602 (2012).
- ⁷M. Takinoue, Y. Atsumi, and K. Yoshikawa, *Appl. Phys. Lett.* **96**, 104105 (2010).
- ⁸T. Kurimura, M. Takinoue, K. Yoshikawa, and M. Ichikawa, *Phys. Rev. E* **88**, 042918 (2013).
- ⁹Y. Jung, H. Oh, and I. S. Kang, *J. Colloid Interface Sci.* **322**, 617-623 (2008).
- ¹⁰D. J. Im, J. Noh, D. Moon, and I. S. Kang, *Anal. Chem.* **83**, 5168-5174 (2011).
- ¹¹M. M. Ahn, D. J. Im, and I. S. Kang, *Analyst* **138**, 7362-7368 (2013).
- ¹²X. Wang, Y. Liu, and Y. Zhang, *J. Dispersion Sci. Technol.* **36**, 893-897 (2015).
- ¹³C. M. Phan, *J. Phys. Chem. Lett.* **5**, 1463-1466 (2014).
- ¹⁴See supplementary material at <http://dx.doi.org/10.1063/1.4958657> for a video of the rotary motion of plastic particles.
- ¹⁵R. Yamamoto, D. Yamamoto, S. Shioi, S. Fujii, T. Kurimura, and K. Yoshikawa, *J. Soc. Powder Technol., Jpn.* **51**, 823-827 (2014).
- ¹⁶W. Kim, J. C. Ryu, Y. K. Shu, and K. H. Kang, *Appl. Phys. Lett.* **99**, 224102 (2011).
- ¹⁷H. Sugiyama, H. Ogura, T. Shiojima, and Y. Otsubo, *J. Appl. Fluid Mech.* **6**(3), 405-412 (2013).
- ¹⁸F. Strubbe, A. R. M. Verschueren, L. J. M. Schlangen, F. Beunis, and K. Neyts, *J. Colloid Interface Sci.* **300**, 396-403 (2006).
- ¹⁹J. K. Park, J. C. Ryu, W. K. Kim, and K. H. Kang, *J. Phys. Chem. B* **113**, 12271-12276 (2009).